Thermal transpiration modeling in Knudsen compressors

Vítor Pimentel Aguiar
vitorpaguiar@tecnico.ulisboa.pt

Instituto Superior Técnico, Universidade de Lisboa, Portugal

August 2021

Abstract

In this work, a numerical study of helium flows in microchannels operated in the slip regime was carried out in order to model the phenomenon of thermal transpiration. For this, a numerical work was developed and validated with numerical, analytical and experimental data from other authors. Three distinct geometries were simulated: rectangular; semicircular and multistage microchannels. The performance of the rectilinear microchannel depends only on the dimension ratio (ε) and the temperature gradient. For ε less than 0,05 the semicircular microchannel behaves like a rectangular channel. For higher ε, the pressure and dimensions of the microchannel also influence the Reynolds number. The relative performance of the semicircular microchannel in relation to the rectangular one, increases with the decrease of the temperature gradient, with the increase in pressure and the dimensions of the microchannel. For the range of values used, the maximum increase reached was 36,37%. A curvilinear microchannel was simulated with a rectangular connector, forming a stage, as well as a microchannel with successive stages connected in series. At certain pressures, temperature differences and dimensions, occurs inversion of the direction of flow. However, for higher pressures, temperature differences, dimension ratios and number of stages, the performance of Knudsen compressors improves. The relative performance of these systems, when compared with simple rectangular microchannels, improves the more stages they have, the greater the pressure and the dimension ratio, and the smaller the temperature differences.

Keywords: Knudsen compressor, Thermal creep, Rarefaction, Slip flow regime, Performance, CFD.

1. Introduction

The improvement of the manufacturing techniques of micro-electro-mechanical systems has enabled the development of a greater number of technologies, such as in microfluidic. Thus, scientific interest in these systems has been growing a lot in recent decades. Some of the reasons for the increase in studies on these microsystems are that they have features such as compacity, low weight, reduced energy consumption, and easy coupling to other systems [1]. The possible applications of these systems are numerous, such as: heat exchangers for the cooling of integrated circuits, portable gas chromatographic systems for the detection of pollutants in the air, microreactors of small quantities of hazardous substances and/or expensive, gas flow cytometers [2], and the Knudsen compressor/pump.

Conventional pumps/compressors have the inconvenience of wear due to friction of moving parts, thermal inefficiency, difficulty producing components with a low dimension tolerance, and problems associated with the lubrication of moving parts [3]. In turn, the Knudsen compressor/pump, which operates based on a phenomenon of kinetic nature of rarefied gases, in particular thermal transpiration, does not require mechanical parts or lubricating fluids.

The phenomenon of thermal transpiration was first observed and explained by Reynolds and Maxwell. The multi-stage Knudsen pump was proposed by Knudsen in 1910 [4], where it achieved a compression ratio of 10. Currently, smaller microchannels, made from materials with low thermal conductivity allow to significantly increase the performance of Knudsen compressors [3].

Studies have been conducted on microchannels in recent years. Arkilic *et al.* [5] experimentally studied and developed an analytical model for isothermal flows in rectilinear microchannels with pressure gradients; Méolans *et al.* [6] created an analytical and numerical model for isobaric microflows driven by the phenomenon of thermal transpiration; Leontidis *et al.* [7] built a numerical model for multi-stage Knudsen compressors, simulating flows with temperature gradients; Monsivais *et al.* [8] investigated the phenomenon of thermal creep in the case where the temperature profile on the microchannel wall is not known, analyzing asymptotically and numerically the heat transmission between a microchannel wall and the fluid.

This work aims to study the phenomenon of thermal transpiration in microchannels with different geometries, pressures, and temperature profiles. According to Klein [4], these devices have a higher efficiency when operated as pumps, rather than compressors. It is intended, then, to study the mass flow of each microchannel and describe its relationship with the physical and geometric properties considered in this study.

2. Theoretical foundation

The problem under study is a compressible, steady-state, and non-isothermal flow, fundamental in the dynamics of rarefied gases. This is governed by a set of equations: the law of mass conservation, the conservation of momentum, and the 1st law of thermodynamics (energy conservation). The first two laws enunciated form the Navier-Stokes equations, being adequate to the flows under study. The flow considered is gas, under rarefaction conditions. The degree of rarefaction can be quantified by the number of Knudsen, *Kn*, given by:

$$Kn = \frac{\lambda}{H} \qquad (2.1)$$

λ being the average mean free path of the particles, defined as the average distance they travel until they collide, and H the characteristic dimension of the flow. With the increase of *Kn*, gas rarefaction effects arise, namely viscous slip and thermal transpiration of fluid particles near solid walls, as well as a temperature jump between the wall and fluid particles.

Unlike macroscopic and continuous flow, where *Kn* takes low values and there is no slip on the wall, it turns out that fluid particles adjacent to the wall have a non-zero tangential velocity. In the presence of temperature gradients in solid walls, fluid particles are moving towards the thermal gradient. Figure 1 qualitatively describes the phenomenon of thermal transpiration: the collision in the wall of the blue and red particles results in a force in the opposite direction to that of the thermal gradient. Since the particles in red are at a higher temperature, they transfer a greater momentum. By Newton's third law, it follows that the wall exerts a force on the particles in the opposite direction.

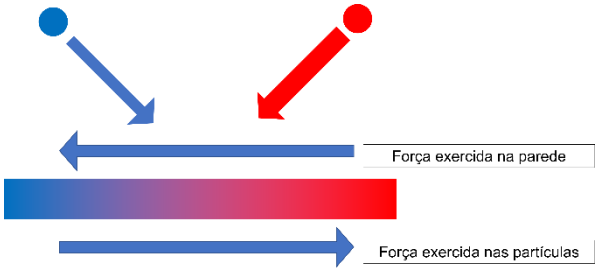

Figure 1- Phenomenon of thermal perspiration. From blue to red, there is an increasing gradient of temperatures. Adapted from [4].

In this work, the flows are operated within the slip regime, with $0{,}01 < Kn < 0{,}1$. In this regime, the effects of rarefaction are accentuated in a layer close to the wall, called the Knudsen layer, which is comparable to the order of magnitude of the mean free path of particles (λ) [9].

In this layer there is a thermodynamic imbalance because the rate of collision between particles is lower than the rate of collision of particles with the wall [1]. The rarefaction of the gas in regions very close to the wall produces macroscopic effects that makes the velocity and temperature comparable with the same as the external flow to the Knudsen layer. Therefore, it is necessary to consider in the Navier-Stokes equations the boundary conditions that allow to account for the effects of the velocity and temperature field. Figure 2 represents the actual velocity of the gas within the Knudsen layer (full line) and the slip velocity (dashed line), this being a fictitious velocity obtained by a linear extrapolation of the velocity profile of the outer flow to the Knudsen layer towards the wall, which approximates the actual velocity profile.

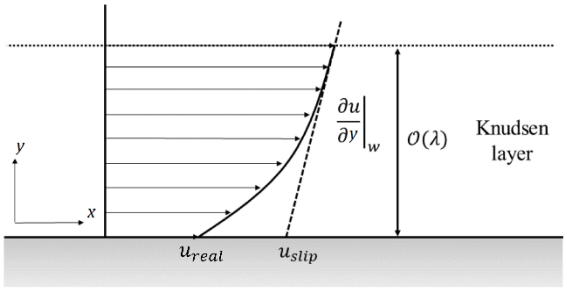

Figure 2- Representation of the velocity profile in the Knudsen layer. u_{real} is the actual speed of the gas and u_{slip} slip velocity. Adapted from [1].

Maxwell proposed for the longitudinal velocity profile on the wall, a boundary condition in the form of the equation (2.2); transverse velocity is zero since there can be no penetration of fluid particles into the wall. In turn, Von Smoluchowski proposed a boundary condition for the temperature jump between the gas and the wall (eq. (2.3)) [1, 10, 11, 12, 13]. For channels with rectilinear walls, the boundary conditions are given by:

$$u_{slip} - u_w = \sigma_P \lambda \left(\frac{\partial u}{\partial y}\right)_w + \sigma_T \frac{\mu}{\rho T_{gás}} \left(\frac{\partial T}{\partial x}\right)_w \qquad (2.2)$$

$$T_{gás} - T_w = \xi_T \lambda \left(\frac{\partial T}{\partial y}\right)_w \qquad (2.3)$$

For complex geometries, such as curved walls, it is necessary to adopt the full stress tensor [13, 7].

The coefficients of the boundary conditions (eq. (2.2), (2.3)) can be calculated using the model proposed by Maxwell, in which they depend on the Tangential Momentum Accommodation Coefficient (TMAC - σ_v). This allows to describe the interactions between the gas particles and the wall surface. The TMAC takes values between 0 and 1 and represents the probability of a particle reflecting diffusely after colliding with the wall.

By this model, the coefficients are approximated as follows:

$$\sigma_P = \frac{2-\sigma_v}{\sigma_v} \quad (2.4)$$

$$\sigma_T = \frac{3}{4} \quad (2.5)$$

$$\xi_T = \frac{2-\sigma_v}{\sigma_v}\frac{2\gamma}{Pr(\gamma+1)} \quad (2.6)$$

3. Numeric model implementation

A numerical model was developed, performing the verification and validation of the models, to obtain the results of section 4.

The program used was COMSOL Multiphysics [14]. This has a wide variety of physical models to simulate the various problems encountered in the most diverse branches of engineering. The method of discretization used by the software is the Finite Element Method that allows the initialization of the resolution of the system of equations and the Newton's method approximates the solution to the exact one.

Numerical models were developed that reproduced the domain and boundary conditions of the studies of Arkilic *et al*. [5], Méolans *et al*. [6] and Leontidis *et al.* [7]. The verification was performed for each study, selecting the meshes that produced accurate results and that were not computationally demanding.

The validation of the numerical model was achieved by comparing the results of the authors with the results of this study, obtaining small deviations.

4. Results

This section presents the results obtained by the numerical model used for various geometries, where parametric studies were made with various parameters that can influence the performance of microchannels. The impact they have was studied, to know the configurations that maximize the potential of microchannels. All the results in this chapter were obtained with invariant boundary conditions in time; the pressure boundary conditions at the inlet and outlet are identical, so the flow is driven only by the phenomenon of thermal transpiration. Helium flow was studied in all cases.

4.1. Rectilinear Microchannel

It is intended to verify if there are differences in the mass flow and/or Reynolds number when doing a parametric study of the thickness and length of the microchannel. A parametric study was conducted for the pressures of 1 and 8 atm, for thicknesses H of 1 up to 8 μm, considering as an independent variable the ratio of dimensions. It was considered that the channel entrance is at $300K$, and the difference in temperature at the ends of the channel is also $300K$.

The results are shown in figure 3, where you get several curves overlapping each other. Thus, the Reynolds number is only a function of the dimension ratio, not depending on the pressure nor the dimensions of the microchannel. For equal ratios of dimensions, and for different dimensions, the Reynolds number remains the same because when scaling the length by one factor, the temperature gradients are proportional to the inverse of the same factor, as well as the velocity. To maintain the same value of ε, the height of the microchannel H it must be scaled in the same way, and so the Reynolds number remains the same, since there is a cancellation of proportions.

It is thus concluded that the Reynolds number depends exclusively on the parameter ε, so it is possible to do a parametric study by varying both parameters of the microchannel dimensions, or only one of them (H or L). It should be noted that this phenomenon occurs because the temperature intervals (ΔT) are the same for all dimensions used, and thus the gas properties remain constant in the microchannel.

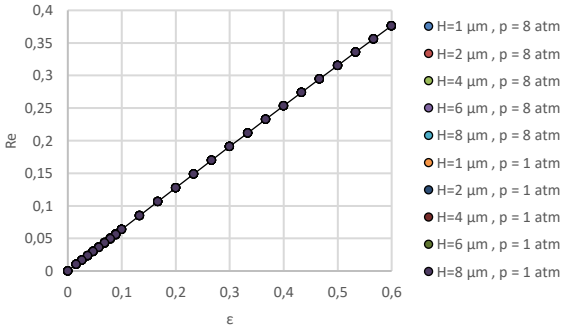

Figure 3 - Reynolds number curves as function of the ratio of dimensions, for different thicknesses and pressures. Obtained with a difference in temperature of 300K.

The Reynolds number was studied as a function of the ratio of dimensions (ε) and temperature differences. Like all variables that Re_i includes are related to the temperature at the output, it can be concluded that the increase in ΔT causes a change in the variables so that Re_i increases. It is understood that the increase in thermal creep implies an increase in velocity, which is superior to the combined effect of the decrease in density and the increase in viscosity, increasing the Reynolds number. It turns out again that Re_i grows linearly with the ratio of dimensions, which is expected, since for shorter lengths (larger ε) the thermal gradient is higher, increasing the flow speed. These behaviors are observable in figure 4.

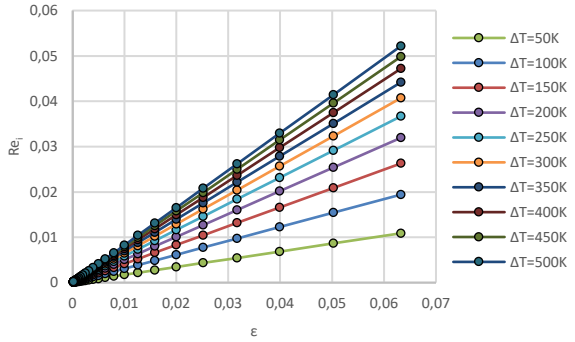

Figure 4 - Reynolds number curves as function of the ratio of dimensions ε, for various temperature differences. Obtained for the pressure of 1 atm.

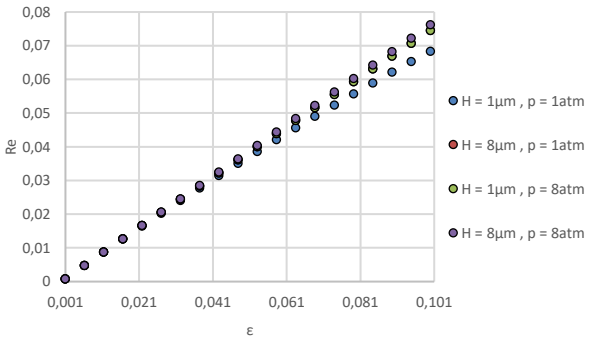

Figure 6 - Reynolds number data as a function of the ratio of dimensions, thickness, and flow pressure, obtained for a temperature difference of 300K. The grey and orange dots are overlapping due to the similarity of the flows.

4.2. Curvilinear Microchannel

It was now considered a semicircular geometry as represented in figure 5, to study the effect of curvature on the flow. The same analysis used for the rectangular channel was applied, where the effect of pressure, temperature variation and microchannel dimensions was studied, comparing simultaneously the results of both geometries. This analysis allows us to understand the conditions in which the performance of the curvilinear microchannel is superior to that of the rectilinear microchannel.

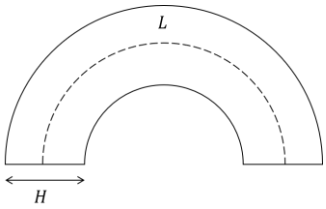

Figure 5 – Geometry of the curvilinear microchannel, H and L being the thickness and length of the microchannel axis, respectively.

A study of geometric parameters was carried out over the flow. Thus, it is intended to check how ε affects the Reynolds number, since for larger ratios of dimensions the curvature of the microchannel is more expressive.

In this in-depth analysis, the study was carried out for ratios of dimensions between 10^{-3} and 10^{-1}. Flows were simulated for channel thicknesses of 1 and 8 μm, operating at pressures of 1 and 8 atm, maintaining the same temperature variation between the input and output of the microchannel ($300K$), and the inlet temperature is maintained at $300K$.

Figure 6 presents the Reynolds number depending on the ratio of dimensions for the combinations of the two thicknesses and the two pressures. It is observed that for ratios of dimensions less than 0,05, the Reynolds number is only a function of the dimension ratio. For values greater than 0.05, there is a deviation of the curves, thus demonstrating that the Reynolds number is a function of the pressure and microchannel dimensions for larger ratios. It is also verified that, for any condition, the Reynolds number tends to increase with the increase in the ratio of dimensions.

The increase in curvature has greater influence on the flow for higher ratio of dimensions, then it was decided to analyze the flow in the ε interval between 0,1 and 0,6.

Figure 7 represents the behavior of the Reynolds number depending on the ratio of dimensions, channel thickness and two pressures, 1 *atm* (figure 7a) and 8 *atm* (figure 7b). The dashed line denotes the rectilinear channel solution, which allows to compare the solutions of both microchannels. Under the conditions of the figure 7a, the rectilinear microchannel is always superior in terms of Reynolds number. It is also verified that each curve has a maximum value of the Reynolds number, and it is for higher ratios of dimensions, the greater the thickness of the channel. This is because the increase of thickness H and the length L in the same proportion (ε constant), the Reynolds number does not reach the maximum due to the negative influence that the length creates on the thermal gradient.

In case *b* of the same figure, where the pressure is increased to 8 *atm*, the curved microchannel performs better or equal than the rectilinear one, for the entire range of ε considered, and thicknesses greater than or equal to 4 μm. It is also observed that the Reynolds number values are higher for a pressure of 8 *atm*. In addition, it can be noted that in this case, the curves also have maximum of *Re*, which in turn are for higher ε the greater the thickness and pressure is.

The conclusions drawn from the figure 7 are exactly the same for the figures 8 and 9, when the thickness, dimension ratio and pressure are changed.
From figure to figure, the increase in the temperature difference causes a general gap between the curves of the curvilinear channel and the rectilinear channel, and therefore the Reynolds number quotient between the rectilinear and curvilinear microchannel also increases. Nevertheless, the increase in ΔT causes an increase in the Reynolds number for both channels.

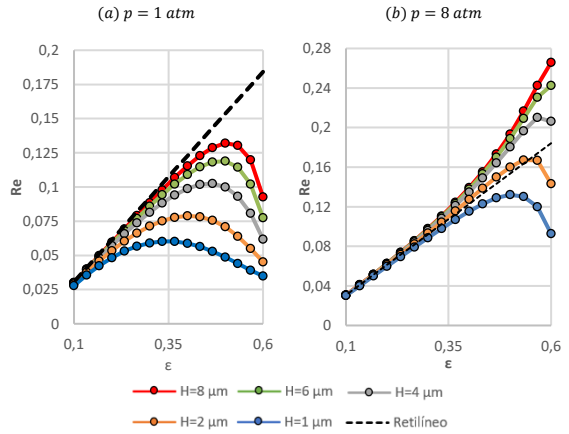

Figure 7 - Reynolds number curves as a function of the ratio of dimensions and channel thickness, obtained for a temperature difference of 100K, and at two different pressures (cases (a) and (b)).

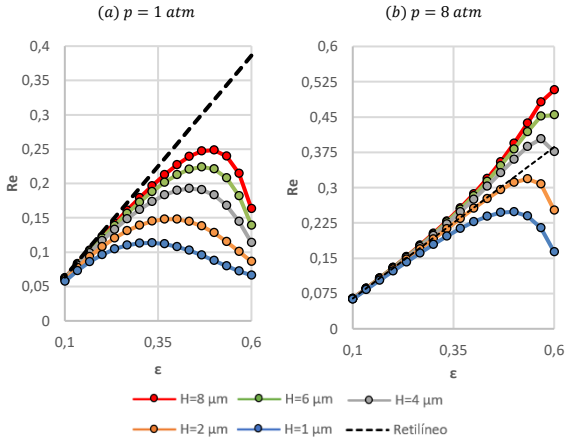

Figure 8 - Reynolds number curves as a function of the ratio of dimensions and channel thickness, obtained for a temperature difference of 300K, and at two different pressures (cases (a) and (b)).

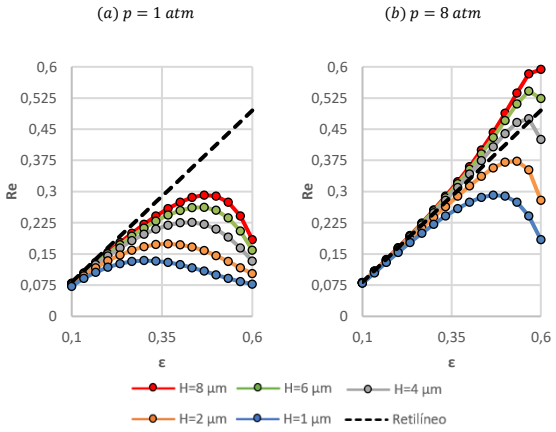

Figure 9 - Reynolds number curves as a function of the ratio of dimensions and channel thickness, obtained for a temperature difference of 500K, and at two different pressures (cases (a) and (b)).

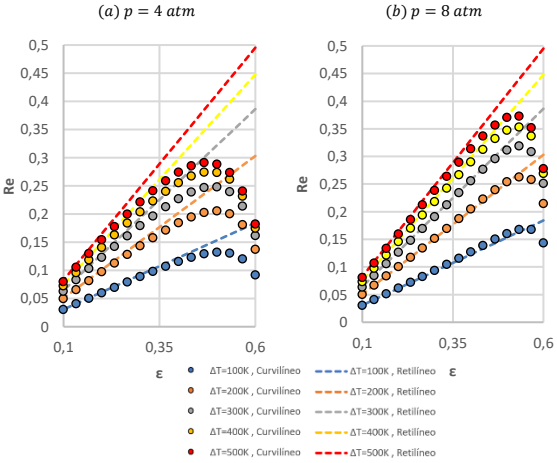

Figure 10 - Reynolds number curves as a function of the ratio of dimensions and temperature differences, obtained with a microchannel thickness of 2 µm.

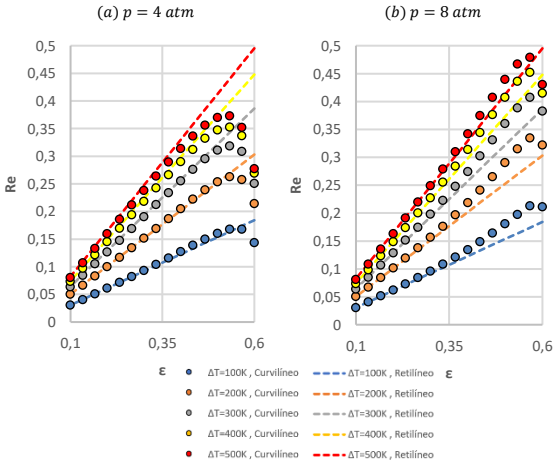

Figure 11 - Reynolds number curves as a function of the ratio of dimensions and temperature differences, obtained with a microchannel thickness of 4 µm.

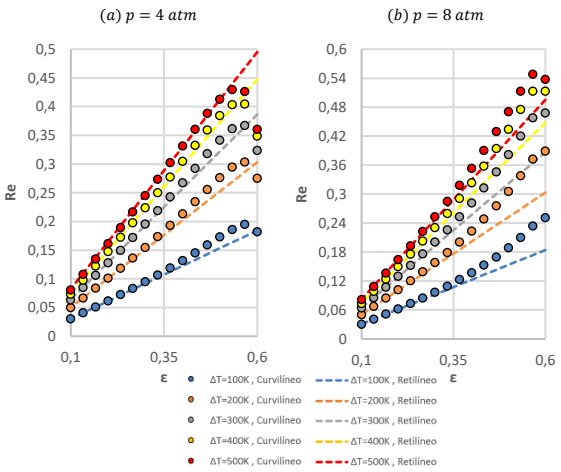

Figure 12 - Reynolds number curves as a function of the ratio of dimensions and temperature differences, obtained with a microchannel thickness of 6 μm.

As it turned out, by increasing the temperature differences the performances of the microchannels improved. Thus, it is useful to study the increases of these performances for varied ΔT, comparing both types of microchannel, rectilinear, and curvilinear. Figures 10, 11 and 12 present the Reynolds number as a function of the ratio of dimensions, for various curves relating to a difference in temperatures, both for the curvilinear channel and the rectilinear channel. The temperature differences used belong to the range of 100 to $500K$, and subfigures (a) and (b) correspond to a pressure of 4 and 8 atm, respectively.

The thickness of the microchannels consecutively was increased from figure to figure, with H equal to 2, 4 and 6 μm. This increase influences positively the Reynolds number, having no effect on the results of rectangular microchannels. The flow pressure similarly affects the Reynolds number for curvilinear channels, having no impact on the results of rectangular channels.

Thus, it is verified that for the lower thickness and pressure values (i.e., $H = 2$ and 4 μm; $p = 4\ atm$) the curves concerning the rectilinear channel generally present a distance from the curves of the curvilinear channel, and the curvilinear channel performance is worse. However, by increasing the thickness and/or flow pressure, the curves of both channels begin to approach in general, and there are specific conditions where there is a turning in the performances of the microchannels, with the curvilinear channel presenting better results.

It is confirmed once again that each curve of the Reynolds number as a function of the dimension ratio has a maximum value of ε higher the greater the thickness H, and pressure. From the graphs it is also concluded that a decrease in the difference in temperature shifts the maximum of the curves to greater ε values.

Figure 10b and figure 11a contain, exactly, the same data for different operating conditions. From figure 10b to figure 11a, there is an increase in thickness by a factor of 2, while the pressure decreases by the same factor. Thus, for the same temperature differences there is a preservation of the dimensional numbers that govern this type of flow, such as the ratio of dimensions ε and the Knudsen number, Kn. More specifically, the parameter $p\sqrt{HL}$, does not vary from one case to another.

Once described the behaviors of the Reynolds number according to the studied variables for various conditions, from figure 7 to figure 12, it is possible to observe that for the higher ratios of dimensions, the behavior of the Reynolds number tends to decline, except for some particular cases. Taking into account the geometry of the microchannel, by increasing the dimension ratio, the lower wall begins to shrink until it reaches a maximum value for ε $(\varepsilon \to \frac{2}{\pi})$, where the wall extinguishes at that limit, turning the microchannel into a semicircular geometry as represented in figure 13. In the ε situation close to the limit, although the phenomenon of thermal creep increases when there is a decrease in the length of the channel axis and/or an increase in its thickness, there is a decrease in the Reynolds number. This is because the lower curvilinear wall of the channel affects a much smaller section of the flow, as illustrated in the figure 14.

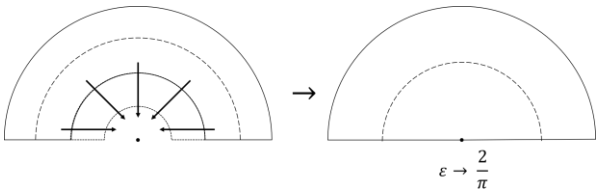

Figure 13 - Illustration of the increase in the ratio of dimensions to the limit of $\frac{2}{\pi}$.

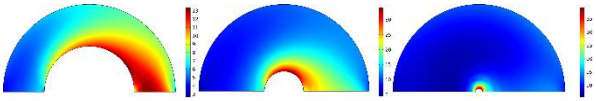

Figure 14 - Illustration of the influence of thermal creep of the lower curved wall when increasing the dimension ratio. The scale represents the magnitude of the velocity vector in m/s.

4.3. Microchannel with connector – Stages

In this section, the flow was studied in a stage consisting of a curvilinear microchannel and a rectilinear section connector, as illustrated in figure 15. It is intended to observe the relationships of the physical properties as well as the impact of the geometry on the flow, to determine if there are characteristic behaviors, which later allows to choose the operating parameters for the

optimization of the Knudsen compressor. The ratio of dimensions for this case encompasses the total axis length of the stage, being defined as:

$$\varepsilon = \frac{H}{2L} \qquad (4.1)$$

A study was carried out for microchannels with a specific set of ratios of dimensions, such as: $\varepsilon = 10^{-3}$; $\varepsilon = 10^{-2}$; $\varepsilon = 10^{-1}$. For ratios of dimensions below 0,1, it was found that the mass flow rate values are very close to zero, which means that the curvilinear microchannel and connector are cancelling the flow relative to each other, and the thermal transpiration in the connector is stronger, which results in the inversion of the flow. For the dimension ratio of 0,1, figure 16 demonstrates mass flow rates that systematically increase with pressure and the dimensions H and L, with H being preponderant. The only conditions represented in which there is inversion of the flow is with the stage of $H = 1\ \mu m$ and pressure of 1 atm.

Since the dimensions have a significant impact on the mass flow and knowing that for considerable ratios of dimensions, the direction of the flow is the desirable and the mass flow takes significant values, the study was continued for dimension ratios of the order of 10^{-1}. Therefore, it is beneficial, for ε in this order, to increase the thickness of the channel and the pressure if they allow to maintain the flow in the slip regime.

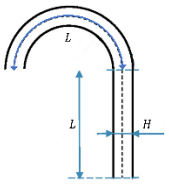

Figure 15 - Geometric representation of a stage used by Leontidis et al. [7] and Aoki et al. [15]. The L and H parameters denote the length of the semi-axis and the thickness of the microchannel, respectively. Adapted from [7].

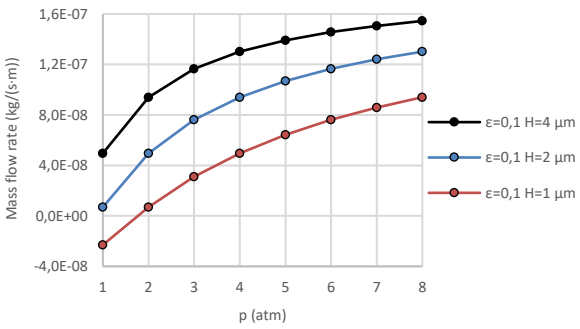

Figure 16 - Mass flow curves as a function of pressure for a dimension ratio of 0,1, and for some microchannel thicknesses. Results obtained with a temperature difference of 600K and the pressure of 1 atm.

Once understood the effect that the ratio of the dimensions, the thickness and length of the stage, have in the flow, the impact of the temperature difference and the pressure on the mass flow rate were analyzed.

Values of the temperature difference between the hot zone (T_H) and the cold zone (T_L) of the microchannel were chosen belonging to the range [100, 600] K, and the pressures considered are between 1 and 8 atm; with $H = 4\ \mu m$; in addition, it was opted for values of ε equal to 0,15; 0,2; 0,25 and 0,3. Figure 17 contains the results only for two ε.

Generically, it is observed that the larger the ε, the greater the mass flow rate, except for some situations: for curves of 1 atm the mass flow decreases continuously when the ratio of dimensions is increased; this is because pressure has more influence for increasingly large dimension ratios. For larger ratios, lower pressures have a higher negative impact on curvilinear microchannel flow. For these reasons, the mass flow of the curvilinear microchannel assembly and the connector begins to decline and may reverse the direction of the flow.

It is possible to note that in cases *a* and *b* of figure 17, there are curves that begin to decline from a certain ΔT. The increase in ΔT causes a decrease in the performance of the curvilinear microchannel compared to the rectilinear one.

Another factor that influences the flow is the reduction of thermal slip on the lower wall of the curvilinear component of the channel.

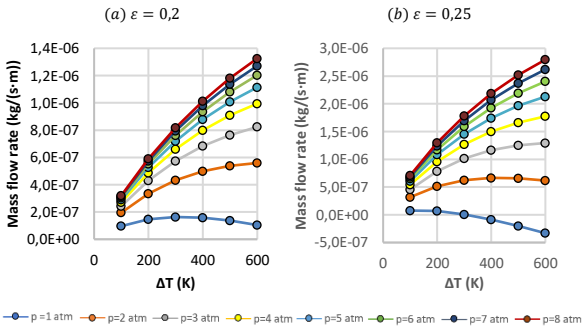

Figure 17 - Mass flow curves as a function of the differences of temperature and pressure for 2 dimension ratios.

4.4. Knudsen Compressor – Multi-Stage

This subsection adds to the performance analysis of the Knudsen compressor the influence of multiple stages. Thus, N stages (2, 4 e 8) in series were considered, with the thickness H of each stage equal to 4 μm, and the ratio of dimensions of each unit, $\varepsilon_{estágio}$, values of 0,15; 0,2 e 0,25.

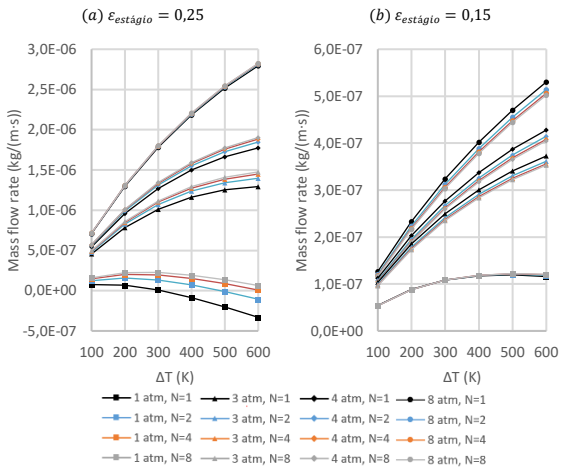

Figure 18 - Mass flow curves as a function of temperature difference, pressure, and number of stages. Obtained for two $\varepsilon_{estágio}$.

By the results of the figure 18a, the increase in the number of stages shows an improvement over the mass flow rate for a dimension ratio of 0,25.

It is observed that there are several factors that influence the mass flow. The increase in temperature difference amplifies the improvement of the mass flow rate when adding stages to the Knudsen compressor, this is observed by the increasing spacing between the curves. Pressure is also a parameter that influences the flow, as when increasing it, the variations of the mass flow rate with the increase in the number of stages become smaller and smaller, and it is not useful to add stages to the pressure of 8 *atm*.

It is important to note that for the pressure of 1 *atm*, and as stated earlier, there are negative mass flow rates, however, the increase in the number of stages has a positive impact, so that the flow acquires the desirable direction. For a Knudsen compressor with $\varepsilon_{estágio} = 0,15$, the increase in the number of stages did not contribute positively to the mass flow rate, as shown in figure 18b. It is also observed the same conclusions drawn earlier in relation to the effect of the temperature difference. After verifying the behavior for the two situations mentioned above, it is verified that there is a pressure, for each ratio of dimensions, from which it is no longer advantageous to add stages to the compressor, and so the shorter Knudsen compressors becoming more beneficial. This pressure is lower, the lower the dimensions ratio.

In short, it is inferred that different ratios of dimensions of each stage have different characteristics, which can be useful depending on the application. For example, for a dimension ratio of 0,25 it is more pertinent to operate the Knudsen compressor at higher pressures, to avoid mass flows in the reverse direction. In the impossibility of operating at pressures other than 1 *atm*, the ratio of dimensions that allows to obtain the maximum of the mass flow is that of 0,2. For the case where the dimension ratio is 0,15, in addition to the mass flow being lower in relation to higher ε, the addition of the number of stages only harms the performance of the Knudsen compressor.

In order to know the dimensions that allow the best performance, it was decided to compare the results of the mass flow between the *N*-stage Knudsen compressor and the simple straight channel, which serves as a reference. In this study, the total length of the Knudsen compressor axis was extracted for the various number of stages, defining a global dimension ratio, ε_{Global}, which is also applied to the rectilinear microchannel, making it comparable to the channels in study. In addition, the performance of these microchannels was estimated by means of the quotient between the mass flow of the Knudsen compressor for a respective number of stages, *N*, and the mass flow of the simple rectangular channel. The operating conditions of pressure and temperature differences (ΔT) are the same for all geometries.

Figure 19 denotes the ratio of mass flow rates of the compressors to various pressures, in which each stage has a ratio of dimensions of 0,25, being operated at a temperature difference of $100K$ (case a) and $600K$ (case b). In case a, for compressors with 4 and 8 stages, they have a better performance than the simple rectilinear channel. As ε_{Global} increases, by reducing the number of stages, it is verified that the performance of the Knudsen compressor is reduced, such that for 2 and 1 stages the compressor with a simple rectangular channel is preferable. When operating the microchannels at higher pressures, performance is maximized, since for straight channels it has already been found that the pressure does not influence the mass flow rate, while for the channels under study in this section, the pressure is a factor of influence. In case b it is observed that an 8-stage Knudsen compressor remains a better option than a Knudsen compressor with a straight channel, for all pressures considered except for 2 *atm*. However, for 4 stages, only the pressure of 8 *atm* presents a performance superior to the unit. This indicates that it is more useful to use higher pressures for these conditions and geometry.

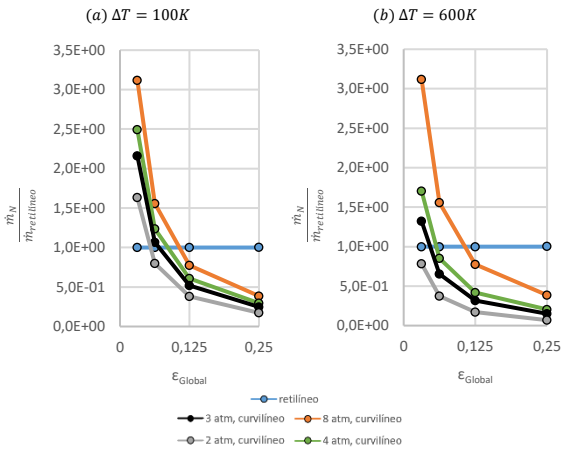

Figure 19 - Mass flow ratio curves between compressor data and simple rectilinear microchannel, $\frac{\dot{m}_N}{\dot{m}_{retilíneo}}$. Results obtained with two temperature differences, and $\varepsilon_{estágio} = 0{,}25$.

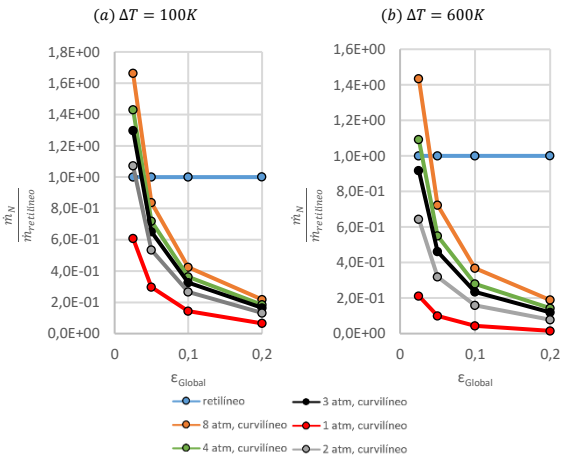

Figure 20 - Mass flow ratio curves between compressor data and simple rectilinear microchannel, $\frac{\dot{m}_N}{\dot{m}_{retilíneo}}$. Results obtained with two temperature differences, and $\varepsilon_{estágio} = 0{,}2$.

Compressor performances with $\varepsilon_{\text{estágio}} = 0{,}2$, are represented in figure 20. For the performances of the case *a,* it is more advantageous to operate compressors with 8 stages at pressures different of 1 *atm*, whereas for 4 or fewer stages it is favorable to use a single rectangular microchannel. In case *b* of the figure, it is observable that the advantage of using this type of channel is limited to 8 stages for pressures greater than 3 *atm*.

Finally, channels that have stages with $\varepsilon_{\text{estágio}} = 0{,}15$, did not present advantages over rectangular microchannels.

Having said that, and analyzing the three cases, it is possible to describe the general behavior of the performance in relation to pressure, temperature, and dimension ratio. In all cases studied, increased pressure increases the performance of all microchannels; with the increase of temperature difference, the performances decrease; lastly, it is inferred that when decreasing the dimension ratio of each stage, from 0,25 to 0,15, the performance also decreases. In general, it can be concluded that the type of channel studied here has a better performance when compared to the straight channel, the more stages it has.

5. Conclusion

This study aimed to study the phenomenon of thermal transpiration in Knudsen compressors, as well as the influence of geometric and physical parameters such as operating temperatures and pressures. For this, a numerical model was developed using the algorithm COMSOL [14]. The numerical model was validated using experimental, numerical, and analytical data from different authors.

Three different geometries were studied operating the microchannels to similar conditions and dimensions.

Regarding the rectangular microchannel, it is concluded that the Reynolds number is a function of the temperature gradient and the dimension ratio, increasing with these variables. This number does not depend on the dimensions of the microchannel nor the pressure, as concluded by Méolans *et al.* [6].

The Reynolds number for the semicircular microchannel is only a function of the dimension ratio and temperature gradient for ε approximately less than 0,05. For higher values, the Reynolds number in general increases with the increase of pressure and thickness of the microchannel. The range of the dimension ratio in which the Reynolds number is decreasing is reduced the higher the flow pressure and the microchannel dimensions. That is, the maximum Reynolds number occurs at ratios of dimensions closer to the limit $\left(\frac{2}{\pi}\right)$. In addition, it was observed that the performance of the curvilinear channel in relation to the rectilinear channel increases, the higher the pressure and thickness of the microchannel, and the lower the temperature gradient, with the largest recorded increase equal to 36,37%.

Finally, the performance of a stage consisting of a curved microchannel and a rectilinear connector was studied. With this geometry, it was concluded that for small-sized ratios ($\varepsilon < 0{,}01$), inversion of the direction of flow occurs for any pressure and thickness considered. The performance of this configuration depends on the pressure and dimensions of the components, and the thickness is decisive in the value of the mass flow rate. It was concluded that the higher the ratio of dimensions, the effect that the pressure has on the flow is amplified, and there is a wider range of pressures for which the direction of flow is reversed. It was also concluded that higher ratios of dimensions show better results, as verified by Leontidis *et al.* [7].

The construction of a multi-stage Knudsen compressor boosts the value of the mass flow rate, with smaller increase for more stages of the compressor. It was observed that, for certain pressure and geometry conditions, the addition of stages aggravates the performance of the compressor. The implementation of more stages benefits the performance of the Knudsen compressor in relation to that of the rectilinear channel, being more profitable the higher the ratio of dimensions of each stage, except for ε very close to the limit $\left(\frac{1}{\pi}\right)$.

Finally, for all the cases studied in which the temperature difference was fixed, it was observed that there are similar flows that only depend on the dimensionless parameters of the Knudsen number and the ratio of dimensions. If the product $p\sqrt{HL}$ remain constant, for the same ΔT, so does the Reynolds number.

References

[1] D. Fratantonio, "Molecular tagging velocimetry in rarefied and confined gas flows," 2019.

[2] R. W. Barber and D. R. Emerson, "Challenges in modeling gas-phase flow in microchannels: from slip to transition," *Heat Transfer Engineering,* vol. 27, p. 3–12, 2006.

[3] Y.-L. Han, E. Phillip Muntz, A. Alexeenko and M. Young, "Experimental and computational studies of temperature gradient–driven molecular transport in gas flows through nano/microscale channels," *Nanoscale and Microscale Thermophysical Engineering,* vol. 11, p. 151–175, 2007.

[4] T. A. Klein, "Energy conversion using thermal transpiration: Optimization of a Knudsen compressor," 2012.

[5] E. B. Arkilic, M. A. Schmidt and K. S. Breuer, "Gaseous slip flow in long microchannels," *Journal of Microelectromechanical systems,* vol. 6, p. 167–178, 1997.

[6] J. G. Méolans and I. A. Graur, "Continuum analytical modelling of thermal creep," *European Journal of Mechanics-B/Fluids,* vol. 27, p. 785–809, 2008.

[7] V. Leontidis, J. Chen, L. Baldas and S. Colin, "Numerical design of a Knudsen pump with curved channels operating in the slip flow regime," *Heat and Mass Transfer,* vol. 50, p. 1065–1080, 2014.

[8] I. Monsivais, J. J. Lizardi and F. Méndez, "Conjugate thermal creep flow in a thin microchannel," *International Journal of Thermal Sciences,* vol. 124, pp. 227-239, 2018.

[9] Y. Sone, Kinetic theory and fluid dynamics, Springer Science & Business Media, 2002.

[10] G. Karniadakis, A. Beskok and N. Aluru, Microflows and nanoflows: fundamentals and simulation, vol. 29, Springer Science & Business Media, 2006.

[11] E. H. Kennard and others, Kinetic theory of gases, vol. 483, McGraw-hill New York, 1938.

[12] M. N. Kogan, "Flows at Small Knudsen Numbers," in *Rarefied Gas Dynamics*, Springer, 1969, p. 367–400.

[13] D. A. Lockerby, J. M. Reese, D. R. Emerson and R. W. Barber, "Velocity boundary condition at solid walls in rarefied gas calculations," *Physical Review E,* vol. 70, p. 017303, 2004.

[14] *Simulate real-world designs, devices, and processes with multiphysics software from COMSOL..*

[15] K. Aoki, P. Degond, L. Mieussens, S. Takata and H. Yoshida, "A diffusion model for rarefied flows in curved channels," *Multiscale Modeling & Simulation,* vol. 6, p. 1281–1316, 2008.